Indian Journal of Fibre & Textile Research
Vol. 49, December 2024, pp. 470-478
DOI: 10.56042/ijftr.v49i4.6148

Hydraulic conductivity of porous media consisting of natural fibres for drainage applications

Temesgen Regassa Woyessa[1,a], R Chattopadhyay[1] & G V Ramana[2]

[1]Department of Textile and Fibre Engineering, [2]Department of Civil Engineering, Indian Institute of Technology Delhi, New Delhi 110 016, India

Received 12 October 2023; revised received and accepted 18 March 2024

In the present study, the hydraulic conductivities of coir, jute, and kenaf fibre assemblies are thoroughly investigated, along with polypropylene fibres. The fibres are first parallelized through repeated combing and then converted into a sliver using suitable carding machines. The parallelized fibres are inserted into a sample holder (PVC tube). The hydraulic conductivity of the fibrous bundles is evaluated by following ASTM D4716, at porosity (φ) 0.8, 0.90, and 0.95; and the hydraulic gradient (i) 0.5, 1, and 2.5. The hydraulic property of fibres in bundle form largely depends on the porosity of the fibrous structure. For similar porosity, a medium consisting of larger diameter fibres facilitates easy liquid flow.

Keywords: Coir fibre, Geotextiles for drainage, Hydraulic conductivity, Jute fibre, Kenaf fibre, Porosity

1 Introduction

The hydraulic property of geotextiles is essential when it works as a filter or drainage medium. Geotextiles act as drains by collecting and redirecting liquids away from the affected areas. Drainage applications are predominantly used in pavement layers, highway embankments, and soft ground improvements. Draining water from soft soil can facilitate consolidation and stabilize the structure. Geotextiles retain soil particles while allowing water to pass through their pores during drainage, a process known as filtration. Both filtration and drainage are critical functions, requiring water to pass through the geotextile drain structures in one of three directions: across, along, or a combination of both.

The permeability of the geotextiles is a crucial property in drainage applications. It can be affected by factors such as fibres' physical properties (linear density, diameter, diameter uniformity, shape factor), physical properties of the geotextile (mass per unit area, thickness, packing coefficient), porosity (pore size and distribution), fibre arrangement, external stress, hydraulic gradient, and fibre type (natural or synthetic)[1–4].

Fibres suitable for geotextile for drainage applications should have the right combination of mechanical, chemical, and hydraulic properties. Synthetic fibres such as polypropylene, polyethylene, and polyester are widely used for drainage applications due to their long service life, lower weight, and efficient functioning. However, natural fibres have an advantage over synthetic fibres in biodegradability, easy availability, and lower cost. Coir, jute, and sisal are among the most commonly used natural fibres. Coir fibres, in particular, are stiffer, extendable, and decompose slowly in soil compared to other natural fibres.

According to Nguyen and Indraratna (2016)[5], coir, with its larger average diameter than jute fibres, is expected to have greater hydraulic conductivity. A coir fibre with more uniform or lower size dispersion (27·1%) experiences higher hydraulic conductivity than jute fibres with low uniformity or higher size dispersion (40.3%). The finer the fibres, the less will be the channel diameters, leading to more resistance to flow, and hence decreased permeability[2,5].

Jute fibres with a non-circular shape, have a larger shape factor, which results in a larger fluid-fibre contact area, making jute fibres less permeable than coir fibres with an almost rounded cross-sections. The fibrous bundles' hydraulic conductivity also influence the fluid-particle interaction forces[6]. The fibres' orientation gets disturbed by a larger fluid interaction force exerted on the fibres. To avoid the disturbance of the fibrous assembly by fluid pressure, fluid flow in the fibrous materials should be in a laminar flow state. The hydraulic permeability of cocoons made from coir fibre decreased as the density of the fibrous assembly increased[3].

[a]Corresponding author.
E-mail: tameiitd@gmail.com

Nonwoven geotextiles are commonly utilized in drainage, but their compressibility leads to rapid decline in their permeability. Geo-composites, which are relatively compression resistant, are widely employed in long-term drainage applications.

The drainage properties of the geotextiles can be evaluated under saturated or unsaturated conditions[7]. In saturated conditions, running water is used, while under unsaturated conditions, it is assessed by transmissivity under suction[8] or wetting-wicking (capillary action) principles[9,10]. Methods like in-plain permeability[11] and cross-plain permeability[12] evaluate drainage properties under saturated conditions, while vertical and horizontal wicking tests assess drainage under unsaturated conditions.

Since synthetic fibres are not biodegradable, the demand for natural fibre geotextiles is increasing in applications such as prefabricated vertical drains (PVD), soil stabilization in road construction, protection of hill slopes, river banks, etc. However, prior studies have been limited to coir and jute fibres only. In the present study, the hydraulic conductivity of coir, jute, and kenaf fibre assemblies have been thoroughly investigated along with polypropylene (PP) fibres. PP fibre has been chosen with a view to compare the performance of natural and synthetic fibres.

2 Materials and Methods

2.1 Materials

Coir, jute, kenaf, and polypropylene fibres were used in this study. The diameter of the jute fibres ranged from 10 μm to 110 μm with an average of 46.43 μm, consistent with the results reported in previous studies[5,13,14]. Similarly, the diameter of coir fibres varied between 40 μm and 280 μm, with an average of 104.01 μm, aligning with previous literature[5,14]. Kenaf fibres exhibited diameters ranging from 30 μm to 130 μm, with an average of 70.00 μm, which agrees with previously reported values[14,15]. The average diameter of polypropylene fibres was 48.00 μm.

2.2 Methods

2.2.1 Sample Preparation

Jute and kenaf fibres were mechanically opened and individualized using a carding machine designed for processing bast fibres. Polypropylene fibres were opened using a laboratory model carding machine designed for processing synthetic fibres. Coir fibre, being coarse, did not require opening and individualization. Coir, jute, and kenaf fibres were first parallelized by repeated combing and then converted into a sliver using a Gill-box machine. The parallelized fibrous assembly was slowly inserted into a sample holder (PVC tube with a diameter of 1.27 cm and length of 14.5 cm). The sample holder filled with fibres (Fig. 1) was taken for further study.

2.2.2 Hydraulic Conductivity

The test was conducted following ASTM D4716. The schematic diagram of the test setup is shown in Fig. 2. The water tank was kept at an elevated height, filled with continuously flowing water. Two valves were located at the inlet and outlet to regulate the water flow. The hydraulic conductivity of the fibrous bundles was evaluated by keeping the porosity and hydraulic gradient at three levels, viz., porosity (φ) at 0.8, 0.90, and 0.95, and hydraulic gradient (i) at 0.5, 1, and 2.5 (Table 1).

Now, both ends of the sample holder containing the parallelized fibrous medium were connected to the flow pipes, which were connected to a manometer for measuring pressure loss. Four valves (V_1, V_2 V_3, and V_4) regulated the flow pressure, released water from the reservoir, and allowed water to pass through.

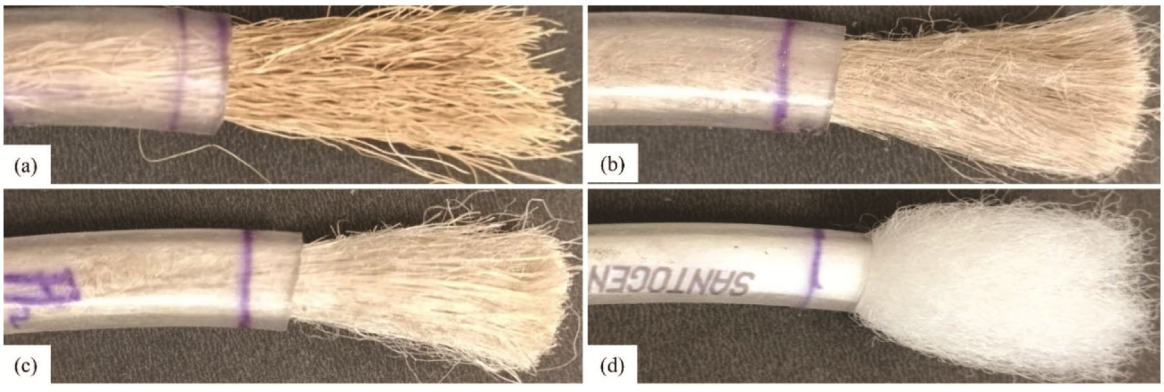

Fig. 1 — Sample within PVC tube: (a) Coir fibre, (b) jute fibre, (c) kenaf fibre and (d) polypropylene fibre

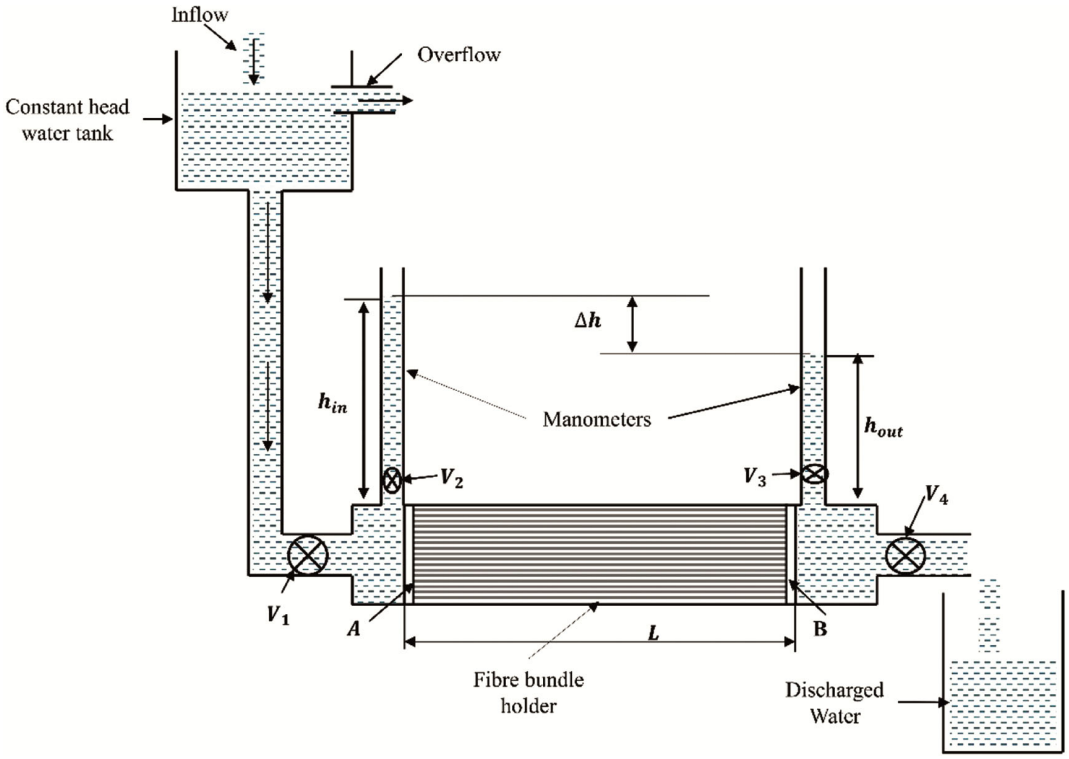

Fig. 2 — Test set-up: (V_1 −inlet valve, V_2 −outlet valve, V_3 & V_4 −valves used to control water rise in the manometers, and A & B − sample holder connectors)

Table 1 — Experimental plan

Run	Sample porosity	Gradient
1	0.80	0.5
2	0.80	1.0
3	0.80	2.5
4	0.90	0.5
5	0.90	1.0
6	0.90	2.5
7	0.95	0.5
8	0.95	1.0
9	0.95	2.5

The mass of fibres (w) within the sample holder ($length - L$) was varied to achieve different levels of porosity. The porosity (φ) was calculated using the following formula:

$$\varphi[\text{-}] = 1\text{-}\frac{\rho_b(g/cm^3)}{\rho_f(g/cm^3)} = 1 - \frac{w/\pi r^2 L}{\rho_f} \quad \ldots(1)$$

where (ρ_f) is the density of fibre; (ρ_b), apparent density of the fibrous medium within the tube; and r, internal radius of the sample holder (6.35 mm). The porosity of the packed medium of fibres was kept at 0.8, 0.9, and 0.95.

Initially, all valves were kept opened, allowing water from the reservoir to flow through the fibrous bundle. The required pressure difference was obtained by adjusting valves V_1 and V_4, altering the water levels in the manometers. Once the pressure difference was achieved, the water was allowed to flow through the fibrous bundles for some time to stabilize the flow. The volume of water discharged was recorded for 30 min at 5 min intervals. The hydraulic conductivities of parallelly arranged fibrous bundles made of coir, jute, kenaf, and polypropylene were calculated.

2.2.3 Hydraulic Parameters

Pressure Drop

The hydraulic pressure (Δh) drop was computed using the difference in liquid heights between the input and output manometers using the following equation:

$$\Delta h(m) = h_{in}(m) - h_{out}(m) \quad \ldots(2)$$

Hydraulic Gradient

The hydraulic gradient (i) was determined by dividing the difference in water pressure (Δh) by the length of the sample holder filled with fibres using the following equation:

$$i[-] = \frac{\Delta h(m)}{L(m)} \quad \ldots(3)$$

where $(h_{in.})$ is the water pressure at the inlet; $(h_{out.})$, the water pressure at the outlet; and (L), the length of the sample tested. Hydraulic gradients of 0.5, 1, and 2.5 were chosen.

Hydraulic Conductivity and Water Discharge Velocity

Following ASTM D4716, flow velocity V_s (m/s) and hydraulic conductivity $k(m/s)$ of the fibrous bundles were calculated using the following equations:

$$V_s(m/s) = \frac{V_w R_T}{A_t t} \quad ...(4)$$

$$k(m/s) = \frac{V_s}{i} = \frac{V_w R_T}{i A_t t} \quad ...(5)$$

$$R_T = \frac{T}{20} = \frac{1.767}{1+0.0337T+0.00022T^2} \quad ...(6)$$

where (A_t) is the interior cross-sectional area of the tube $(1.27\times10^{-4}\ (m^2)$; (V_s), flow velocity; (V_w), the water volume obtained at the outlet; t, time; (k), hydraulic conductivity; (R_T), temperature correction factor to 20 ; and (T), the temperature of the water in degree Celsius. The temperature of the water was 23, and the value of (R_T) was determined according to the equation 6[16].

The Reynolds number of the flow was determined as:

$$R_e = D_f V_s \rho_l / \eta$$

where D_f is average diameter of the fibres; ρ_l, is density of the water; and η, water viscosity. The Reynolds number can range from 0.01 to 8.8, so the flow remains laminar[17].

3 Results and Discussion

The experimental results pertaining to discharge rate, discharge velocity and hydraulic conductivity of the fibrous assemblies are discussed below.

3.1 Water Discharge Rate

In Fig. 3(a), the discharge rate of all fibrous bundles having the same porosity (0.95) is shown over 30 min. Since all the fibrous bundles have the same porosity, the discharge rate is expected to be same. However, the coir fibre bundle consistently shows a much higher discharge rate than the others. The discharge rate depends on the resistance (drag) the liquid experiences while passing through the fibrous medium. Amongst the fibres chosen, coir fibres are coarsest (diameter: 104.01 ±0.45 μm), whereas jute and polypropylene are the finest (diameter: 46.43 μm and 48.00 μm , respectively). As the same weights of fibres were packed into the

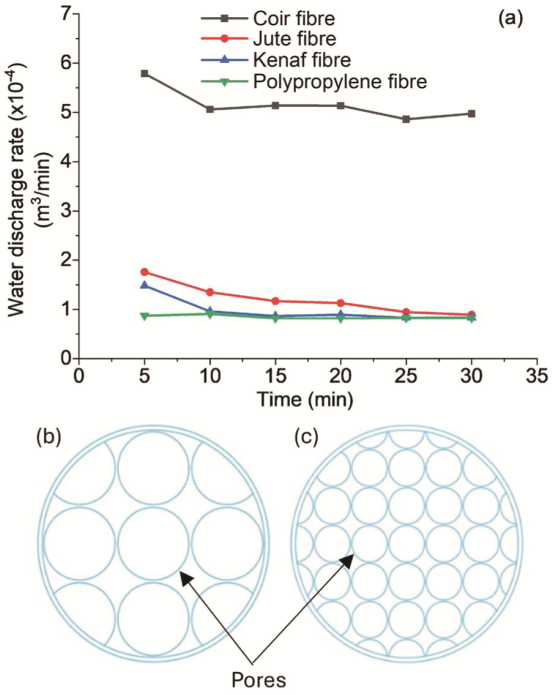

Fig. 3 — Water discharge vs time ($\varphi = 0.95, i = 1$), (b) schematic diagram of coarse fibre arrangement and (c) schematic diagram of finer fibre arrangement

sample holder, the total fibre surface area will be more for finer fibres. The size of the flow channels will also be less for finer fibres. The channels will also be more tortuous in the case of fine fibres as they are more in number. Therefore, many finer channels are created by finer fibres, whereas lesser number of large diameter channels are created by coarser fibres as seen in [Figs. 3(b) & (c)]. Large channels offer less resistance to flow. Thus, discharge rate is less for the jute, polypropylene, and kenaf at any given gradient. Between jute and polypropylene fibres, polypropylene fibres offer more resistance to flow. Being spun under controlled industrial conditions, polypropylene fibres have narrow diameter distribution in comparison to jute and kenaf fibres. On the contrary, jute has a skewed diameter distribution, indicating the presence of many large diameter fibres, which creates large diameter flow channels facilitating easier flow in comparison to polypropylene.

The discharge rate decreases gradually over time for coir, jute, and kenaf fibres, but remains constant for polypropylene fibre [Fig. 3(a)]. The discharge rate of coir fibre medium reduces from 5.79×10^{-4} to $4.97\times10^{-4}\ m^3/min$ (14.16%), while for jute it decreases from 1.74×10^{-4} to $0.89\times10^{-4}\ m^3/min$ (48.73%) and for kenaf from 1.48×10^{-4} to $0.83\times$

$10^{-4}\, m^3/min$ (43.7%). The reduction in discharge rate with time can be ascribed to the swelling phenomenon of the lignocellulosic fibres. The latter absorb water [18] and begin to swell, which decreases porosity and narrows the flow channels. Coir fibre has been reported to swell less (0.1 to 5%)[19] compared to jute fibres (20 to 23%)[20] and kenaf fibre (up to 45%)[21]. As the fibres' diameter continuously increases, the free spaces between the fibres are occupied by the swollen fibres. As a result, the porosity decreases, and the flow channels become narrower. The reduction in porosity creates more resistance to the liquid flow, resulting in a decline in the water discharge rate. As coir fibre swells lesser than jute and kenaf fibres, the drop in water discharge rate is less for coir fibres. Polypropylene fibres, which do not absorb water, maintain a constant discharge rate over time.

3.2 Discharge Velocity

Discharge velocity, the volume flow rate per unit area through the fibrous bundle, was analysed using a 2^2 factorial design experiment with hydraulic gradient and porosity as factors. Hydraulic gradient represents the pressure under which the liquid flows through the medium, and porosity is the fractional void space within the fibrous medium. The experimental plan and the responses for four fibrous bundles are listed in Table 2. The data has been plotted in Fig. 4 for visualization.

Table 2 — Discharge velocity values

Run	Porosity	Gradient	Discharge velocity (m/s) × 10^{-3}			
			Coir	Jute	Kenaf	Polypropylene
1	0.80	0.5	2.07	0.31	0.11	1.41
2	0.80	1.0	2.80	0.59	0.20	1.67
7	0.95	0.5	38.00	4.33	4.63	7.22
8	0.95	1.0	64.30	9.96	9.76	8.81

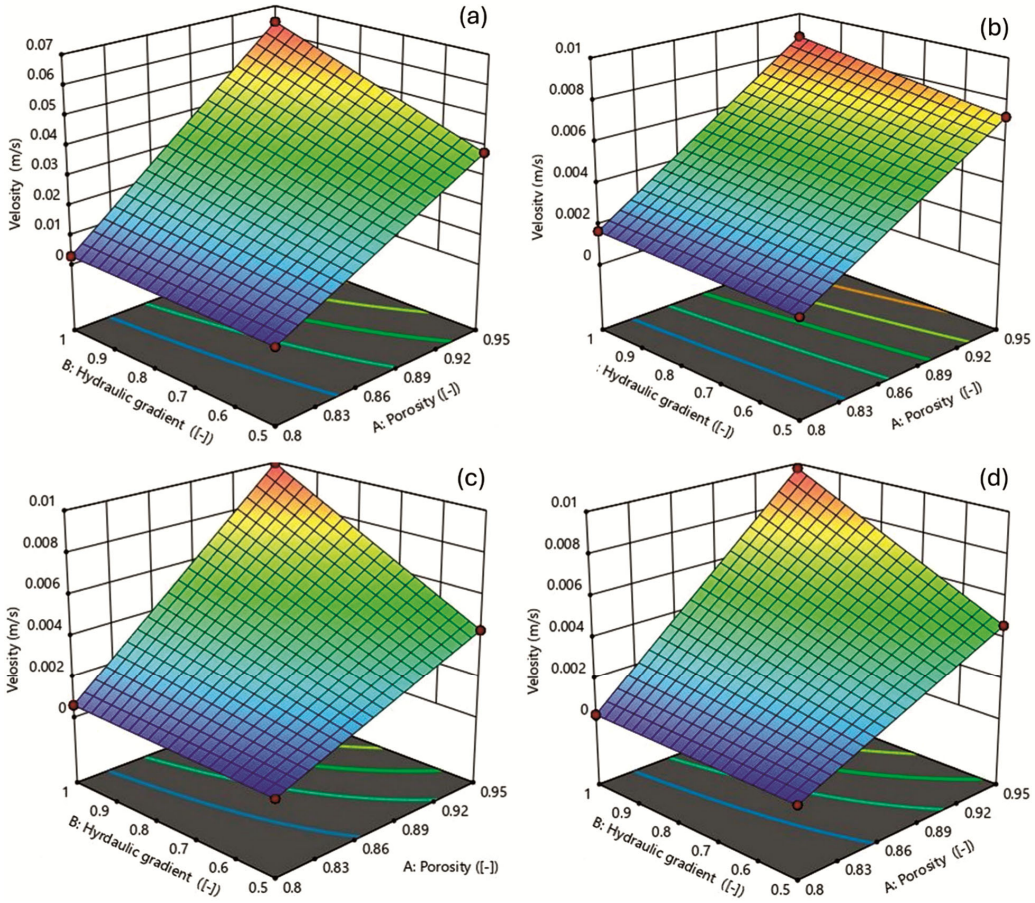

Fig. 4 — Factorial effects of water discharge velocity (a) Coir fibre, (b) polypropylene fibre, (c) jute fibre and (d) kenaf fibre

The following observations can be made:

- discharge velocity increases with an increase in porosity and hydraulic gradient, with porosity having a predominant effect.
- low gradient and low porosity (highly packed fibres) combination results in the lowest discharge
- high gradient and high porosity (lowly packed fibres) combination results in the highest discharge
- coir fibrous assembly shows the highest ischarge velocity followed by polypropylene, jute, and kenaf.

3.3 Hydraulic Conductivity

Hydraulic conductivity (k) indicates discharge velocity per unit gradient or discharge rate/unit area/unit gradient (Eq. 5).

3.3.1Influence of Porosity

Figure 5 shows the hydraulic conductivity as a function of the porosity of the fibrous bundles. The observations are:

- hydraulic conductivity increases as porosity increases irrespective of fibre type.
- coir fibres maintain nearly constant hydraulic conductivity across all hydraulic gradients (i = 0.5, 1, and 2.5).
- jute and kenaf fibres exhibit slightly higher hydraulic conductivities at a hydraulic gradient of 2.5.

Figure 6 compares the hydraulic conductivity of the fibres at a constant hydraulic gradient (i =1) across varying porosity levels (0.8 to 0.95). Coir fibre has better hydraulic conductivity than polypropylene, jute, and kenaf fibres. The hydraulic

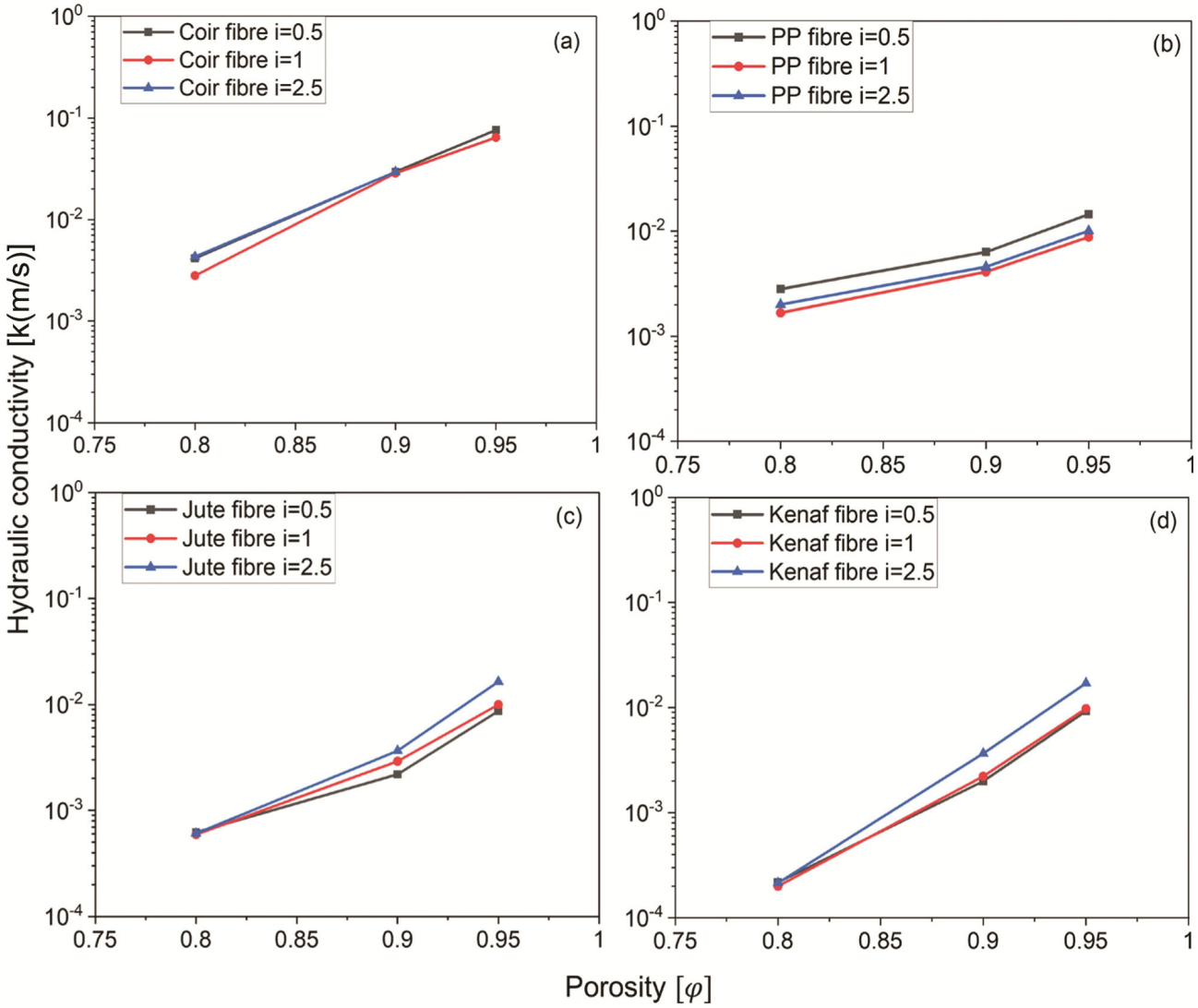

Fig. 5 — Hydraulic conductivity vs porosity (a) Coir fibre, (b) jute fibre, (c) kenaf fibre, and (d) polypropylene fibre

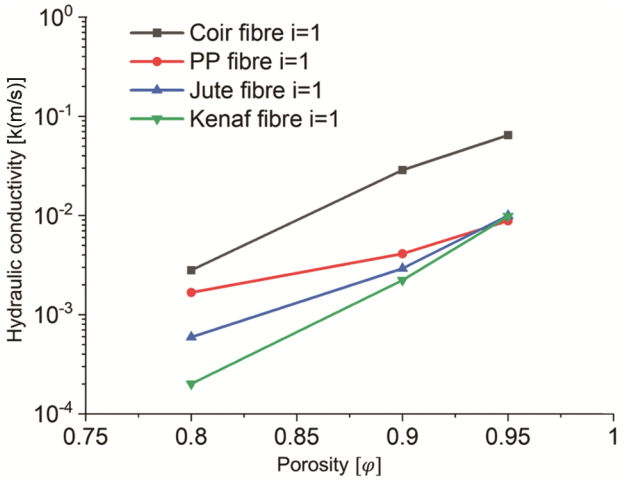

Fig. 6 — Hydraulic conductivity vs porosity

conductivities of jute and kenaf fibres are nearly equal when the porosity (φ) > 0.9. However, at a lower porosity ≤ 0.8, the hydraulic conductivity of jute fibre is greater than kenaf fibre.

As stated earlier, the coir fibre has a larger average diameter than other fibres, creating larger pores and lower resistance to flow compared to the finer fibres, which have a higher specific surface area and more number of small pores. The other factor that may affect the water flow through the porous material is the nature of the material's surface. A rough surface is more resistant to flow than a smoother surface.

3.3.2 Influence of Hydraulic Gradient

Figure 7 plots the hydraulic conductivity of the four fibrous media against hydraulic gradient. The observations are:

- hydraulic conductivity does not change much with increasing hydraulic gradient.
- under identical porosity levels, coir fibrous medium always shows better conductivity than the rest, irrespective of porosity or hydraulic gradient.
- when bundles are tightly packed, i.e., at low porosity ($\varphi = 0.8$), clear-cut differences between the conductivity values of the medium are observed. However, for loosely packed fibres ($\varphi = 0.9$ and 0.95), only the coir fibre medium shows a higher value. Jute, kenaf, and polypropylene fibres have similar values.

The larger flow channels in coir fibres, due to fewer fibres per given mass, contribute to its higher conductivity. The slight drop observed as the gradient is changed from 0.5 to 1.0 is due to the rearrangement of the fibres within the medium due to higher

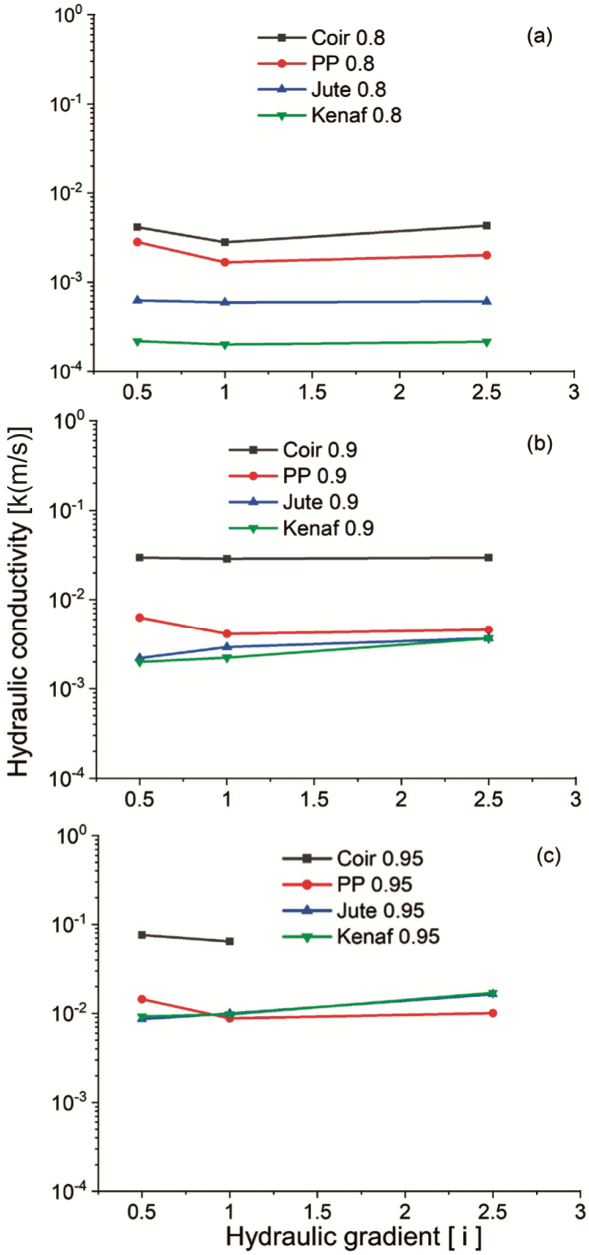

Fig. 7 — Comparison of hydraulic conductivity of fibres (a) φ=0.8, (b) φ=0.9, and (c) φ=0.95

pressure. In the case of coir fibres, at a porosity of 0.95, the experiment could not be conducted as it was impossible to achieve a gradient of 2.5.

The hydraulic conductivity remains practically the same with an increase in hydraulic gradient. Overall, porosity has a greater effect on the hydraulic conductivity of fibrous bundles than the hydraulic gradient, suggesting that porosity optimization is crucial when designing fibrous media for drainage applications.

3.4 Comparison between Predicted and Experimentally Determined Permeability Values

The theoretical permeability values are estimated from analytical models[22–25] as shown in Table 3. The models use parameters such as porosity (φ), fibre diameter (d), and fibre packing coefficient ($\emptyset$). The permeability values of the fibrous medium are calculated with a porosity, $\varphi = 0.9$ and hydraulic gradient, i =1.

The experimental permeability values are calculated using the following formula, as expressed in [26]

$$K(m^2) = \frac{k\eta}{\rho_l g} \quad \ldots(7)$$

where $K$is Permeability (m^2), η, dynamic viscosity of the water at a given temperature $(Kg/m.s)$; ρ_l, density of the water $\left(\frac{Kg}{m^3}\right)$; and g, a acceleration due to gravity (m/s^2). The dynamic viscosity of water at 23℃ is $9.33 \times 10^{-4}(kg/m.s)$. The theoretical and experimental permeability results are shown in Table 4.

The experimentally determined permeability is less than the predicted values based on theoretical models for all fibres (Table 4). This could be due to two reasons: (i) assumption of the flow mediums to be perfectly cylindrical, with larger diameters and parallel alignment and (ii) consideration of small cross-sections of the ideal flow medium. In the experimental evaluation, the flow medium is irregular and consists of discrete fibres. The flow experiences resistance along the fibrous assemblies due to the frictional force between the fluid and the fibre surfaces.

The diameters of all natural fibres vary a lot. The diameter of natural fibres being more irregular results in discontinuous pore channels and reduces hydraulic permeability. For a given mass, fibre diameter decides the specific surface area, which in turn affects the flow resistance. Besides, finer fibres are easy to pack, affecting the pore size between fibres.

Additionally, the cross-sectional shape (shape factor) plays a role. Coir and polypropylene fibres have nearly circular cross-sections, whereas jute and kenaf have irregular cross-sections (Fig. 8). In the coir fibre, a relatively large hole is observed at the center, known as a lacuna[27]. Circular fibre has a shape factor varying between 0 to 0.07, and fibre with an irregular cross section has a shape factor greater than 0.6[28]. A fibre having a large shape factor has a larger fluid-fibre contact area, which increases the fluid drag force between the fibre surface and liquid. It works against the hydraulic conductive property of the fibre.

The theoretical models assume the flow mediums to have a circular cross-section. This could be the

Table 3 — Analytical models by different researchers

Flow media	Permeability equations	References
Annular space between the cylinder	$K = \frac{2 \times \varphi^3 \times d^2}{(1-\varphi)\left[2\ln\left(\frac{1}{1-\varphi}\right) - 3 + 4(1-\varphi) - (1-\varphi)^2\right]}$	22
Parallel permeability of square arrangement	$K = d^2 \times \left(\frac{\pi}{24\emptyset} + \left[\left(\sqrt{\frac{\pi}{4\emptyset}} - 1\right)^3 + 2\right]\sqrt{\frac{\emptyset}{9\pi} - \left(\frac{\pi}{8} + \frac{\emptyset}{8}\right)}\right)\frac{1-\emptyset}{2}$	23
Square arrangement	$K = \frac{0.16 \times d^2 \times \left[\frac{\pi}{4\varphi} - 3\sqrt{\frac{\pi}{4\varphi}} + 3 - \sqrt{\frac{4\varphi}{\pi}}\right]}{\sqrt{1-\varphi}}$	24
	$K = \frac{d^2}{64\emptyset^{1.5}[1 + 56\emptyset^3]}$	25

Note: $\varphi = Porosity, \emptyset = 1 - \varphi$, $\boldsymbol{d}$ =*diameter of the medium/fibre*

Table 4 — Experimental and theoretical permeability

Fibre	Permeability, $K(m^2)$ Experimental	Theoretical Ref. 24	Ref. 25	Ref. 23	Ref. 22
Coir	2.728×10^{-9}	3.856×10^{-9}	1.600×10^{-9}	3.10×10^{-8}	7.90×10^{-8}
Jute	2.766×10^{-10}	7.643×10^{-10}	3.171×10^{-10}	6.11×10^{-9}	1.57×10^{-8}
Kenaf	2.098×10^{-10}	8.21×10^{-10}	3.41×10^{-10}	1.40×10^{-8}	3.58×10^{-8}
Polypropylene	3.911×10^{-10}	8.214×10^{-10}	7.28×10^{-10}	6.57×10^{-9}	1.68×10^{-8}

Table 5 — Permeability ratio (Theoretical /observed results)

Fibre	Experimental	Ratio			
		Ref. 25	Ref. 26	Ref. 24	Ref. 23
Coir	2.728×10^{-9}	1.41	0.58	11.3	28.9
Jute	2.766×10^{-10}	2.76	1.146	22.0	56.7
Kenaf	2.098×10^{-10}	3.91	1.62	66.7	170.6
Polypropylene	3.911×10^{-10}	2.1	1.86	16.7	42.9

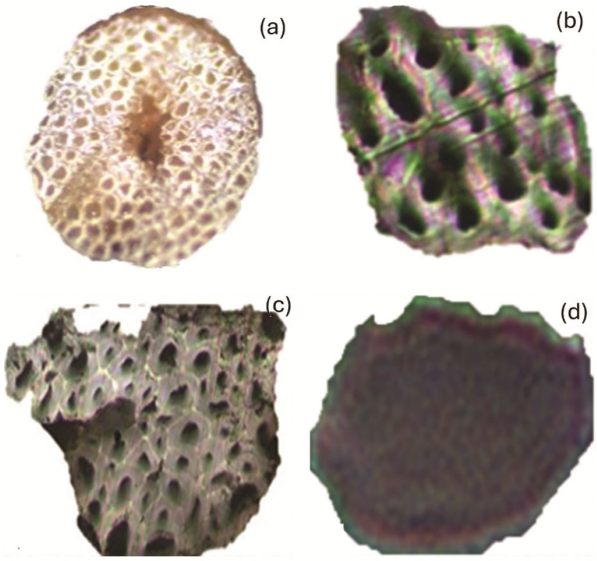

Fig. 8 — Fibres cross-section: (a) Coir fibre, (b) jute fibre, (c) kenaf fibre and (d) polypropylene fibre

reason why jute and kenaf fibres have lower permeability compared to coir and polypropylene.

Among the models, Davie's model provides the most accurate predictions, as it shows the smallest ratio between theoretical and experimental values for all fibres (Table 5). Davies's model is also simpler and more convenient to use compared to other models.

4 Conclusion

From the experimental results and their analysis, several conclusions can be drawn. The water discharge rate of natural fibres, such as coir, jute, and kenaf, gradually decreases over time, while it remains nearly constant for polypropylene fibres. The hydraulic properties of fibres in bundle form are primarily dependent on the porosity of the fibrous medium, emphasizing the importance of optimizing porosity when designing fibrous structures for drainage applications. Additionally, when porosity is constant, larger diameter fibres allow for easier flow. Among the four permeability models compared, Davies's model proves to be the most efficient in predicting the permeability of fibrous structures.

References

1 Williams J G, Morris C E M & Ennis B C, *Polym Eng Sci*, 14 (1974) 413.
2 Hwang G S, Lu C K, Lin M F, Hwu B L & Hsing W H, *Text Res J*, 69 (1999) 565.
3 Indulekha K P, Jayasree P K, Balan K, Dhanesh L & Vinod J S, *J Nat Fibers*, 18 (2021) 2127.
4 Giroud J P, Zhao A & Richardson G N, *Geosynth Int*, 7 (2000) 433.
5 Nguyen T T & Indraratna B, *Proc Inst Civ Engg Ground Improv*, 170 (2017) 123.
6 Nguyen T T & Indraratna B, *Can Geotech J*, 53 (2016)1081
7 Francucci G, Rodríguez E S & Vázquez A, *Compos Part A Appl Sci Manuf*, 41 (2010) 16.
8 Chai J C, In *Geotextiles from Design to Applications* (ed. R.M. Koerner), Woodhead Publlishing, *Ser Text*, 175 (2015) 277.
9 Guo J, Wang F, Zhang X & Han J, *J Mater Civ Eng*, 29 (2017) 1.
10 Lin C & Zhang X, *J Mater Civ Eng*, 30 (11) (2018) 1.
11 ASTMD4716/D4716M-20, (2010) 1.
12 ASTMD4491/D4491M-22, (2012) 1.
13 Virk A S, Hall W & Summerscales J, *Mater Sci Technol*, 25 (2009) 1289.
14 Sathishkumar T P, Navaneethakrishnan P, Shankar S, Rajasekar R & Rajini N, *J Reinf Plast Compos*, 32 (2013) 1476.
15 Samaei S E, Mabadi H A, Mousavi S M, Khavanin A, Faridan M & Taban E, *J Ind Text*, 51 (2022) 8601S.
16 ISO 12958-1, Part 1 (2020).
17 Falkinhoff F, Pierson J, Gamet L, Bourgoin M & Volk R, *Transp Porous Media*, 150 (2023) 285.
18 Mittal M & Chaudhary R, *Int J Appl Eng*, 13 (2018) 12237.
19 Nandan M S, Sai K V, Rakesh P, Kumar N S & Chamberlin K S, *Int J Innov Technol Explor Eng,* 9 (2020) 535.
20 Ghosh S K, *Int J Res Eng Techol*, 03 (2014) 378.
21 Hwang G S, Lu C K, Lin M F, Hwu B L & Hsing W H, *Textile Res J*, 69 (1999) 565.
22 Happel J, *AIChE Journal*, 5 (1959) 174.
23 Tamayol A & Bahrami M, *Int J Heat Mass Transf*, 52 (2009) 2407.
24 Tamayol A & Bahrami M, *Phys Rev E Stat Nonlin Soft Matter Phys*, 83 (2011) 1.
25 Davies C N, *Proc Inst Mech Eng*, 167 (1b) (1953) 185.
26 Russell S J, Woodhead Publishing Limited in assoc. with Textile Inst, (2007).
27 Tran L Q N, Nguyen Minh T, Fuentes C A, Truong Chi T, Van Vuure AW & Verpoest I, *Ind Crops Prod*, 65 (2015) 437.
28 Neckář B & Das D, *Woodhead Publishing India Pvt Ltd*, 7 (2015).